npg

ORIGINAL ARTICLE

Optical tuning of exciton and trion emissions in monolayer phosphorene

Jiong Yang[1]*, Renjing Xu[1]*, Jiajie Pei[1,2]*, Ye Win Myint[1], Fan Wang[3], Zhu Wang[4], Shuang Zhang[1], Zongfu Yu[4] and Yuerui Lu[1]

Monolayer phosphorene provides a unique two-dimensional (2D) platform to investigate the fundamental dynamics of excitons and trions (charged excitons) in reduced dimensions. However, owing to its high instability, unambiguous identification of monolayer phosphorene has been elusive. Consequently, many important fundamental properties, such as exciton dynamics, remain underexplored. We report a rapid, noninvasive, and highly accurate approach based on optical interferometry to determine the layer number of phosphorene, and confirm the results with reliable photoluminescence measurements. Furthermore, we successfully probed the dynamics of excitons and trions in monolayer phosphorene by controlling the photo-carrier injection in a relatively low excitation power range. Based on our measured optical gap and the previously measured electronic energy gap, we determined the exciton binding energy to be ~0.3 eV for the monolayer phosphorene on SiO_2/Si substrate, which agrees well with theoretical predictions. A huge trion binding energy of ~100 meV was first observed in monolayer phosphorene, which is around five times higher than that in transition metal dichalcogenide (TMD) monolayer semiconductor, such as MoS_2. The carrier lifetime of exciton emission in monolayer phosphorene was measured to be ~220 ps, which is comparable to those in other 2D TMD semiconductors. Our results open new avenues for exploring fundamental phenomena and novel optoelectronic applications using monolayer phosphorene.

INTRODUCTION

Phosphorene is a recently developed two-dimensional (2D) material that has attracted tremendous attention owing to its unique anisotropic manner[1–6], layer-dependent direct band gaps[7,8], and quasi-one-dimensional (1D) excitonic nature[9,10], which are all in drastic contrast with the properties of other 2D materials, such as graphene[11] and transition metal dichalcogenide (TMD) semiconductors[12–14]. Monolayer phosphorene has been of particular interest in exploring technological applications and investigating fundamental phenomena, such as 2D quantum confinement and many-body interactions[9,15]. However, such unique 2D materials are unstable in ambient conditions and degrade quickly[8,16]. Particularly, monolayer phosphorene is expected to be much less stable than few-layer phosphorene[16], hence making its identification and characterization extremely challenging. There is a huge controversy on the identification of very few-layer (one or two layers) phosphorene and thus on their properties[16–18]. This controversy was primarily due to the lack of a robust experimental technique to precisely identify the monolayer phosphorene. Consequently, many important fundamental properties of monolayer phosphorene, such as its excitonic nature, remain elusive. In this study, we propose and implement a rapid, noninvasive,

and highly accurate approach to determine the layer number of mono- and few-layer phosphorene by using optical interferometry. The identification is clearly confirmed by the strongly layer-dependent peak energies in the measured photoluminescence (PL) spectra. More importantly, we successfully probed the exciton and trion dynamics in monolayer phosphorene by controlling the photo-carrier injection at a very low excitation power range. The exciton binding energy of monolayer phosphorene on a SiO_2/Si substrate was determined to be ~0.3 eV; this result agrees well with the theoretical prediction that substrate screening strongly affects the exciton binding energy in monolayer phosphorene[15]. Furthermore, a high trion binding energy of ~100 meV (upper bound) was observed in the monolayer phosphorene on a SiO_2/Si substrate, which, again, agrees well with our theoretical calculation. In addition, time-resolved PL (TRPL) was used to characterize the critical carrier dynamics in monolayer phosphorene. The carrier lifetime of exciton emission in monolayer phosphorene was measured to be ~220 ps, a value comparable to those in other TMD semiconductors. Our results provide a new platform for the investigation of fundamental many-body interactions and to explore new optoelectronic applications using monolayer phosphorene.

[1]Research School of Engineering, College of Engineering and Computer Science, The Australian National University, Canberra, ACT 0200, Australia; [2]School of Mechanical Engineering, Beijing Institute of Technology, Beijing 100081, China; [3]Department of Electronic Materials Engineering, Research School of Physics and Engineering, The Australian National University, Canberra, ACT 0200, Australia and [4]Department of Electrical and Computer Engineering, University of Wisconsin, Madison, WI 53706, USA
*These authors contributed equally to this work
Correspondence: Y Lu, E-mail: yuerui.lu@anu.edu.au

MATERIALS AND METHODS

Sample preparation and characterization

Mono- and few-layer phosphorene, graphene, and TMD semiconductor samples were mechanically exfoliated from bulk crystals and drily transferred onto SiO_2/Si (275 nm thermal oxide) substrates. A phase shifting interferometer (Vecco NT9100) was used to obtain all the optical path length (OPL) values for phosphorene samples. Monolayer phosphorene samples were put into a Linkam THMS 600 chamber and the temperature was set as −10 ℃ during the power-dependent PL and TRPL measurements. The power-dependent PL and TRPL measurements were conducted in a setup which incorporates μ-PL spectroscopy and a time-correlated single photon counting (TCSPC) system. A linearly polarized pulse laser (frequency doubled to 522 nm, with 300 fs pulse width and 20.8 MHz repetition rate) was directed to a high numerical aperture (NA = 0.7) objective (Nikon S Plan 60×). PL signal was collected by a grating spectrometer, thereby either recording the PL spectrum through a charge coupled device (CCD; Princeton Instruments, PIXIS) or detecting the PL intensity decay by a Si single-photon avalanche diode (SPAD) and the TCSPC (PicoHarp 300) system with a resolution of ~40 ps.

For few-layer phosphorene (2L to 5L), the PL measurements were conducted using a T64000 micro-Raman system equipped with a InGaAs detector, along with a 532 nm Nd:YAG laser as the excitation source. For all the PL measurements for 2L to 5L phosphorene samples, the sample was placed into a microscope-compatible chamber with a slow flow of protection nitrogen gas to prevent sample degradation at room temperature. To avoid laser-induced sample damage, all PL spectra from two- to five-layer phosphorene were recorded at low power level of P ~20 μW.

Numerical simulation

Stanford Stratified Structure Solver (S4)[19] was used to calculate the phase delay. The method numerically solves Maxwell's equations in multiple layers of structured materials by expanding the field in the Fourier-space.

RESULTS AND DISCUSSION

Both atomic force microscopy (AFM) and Raman spectroscopy have been used to reliably determine the sample thickness of TMD semiconductors with monolayer precision[20]. However, these two methods are not reliable for the identification of very-few-layer phosphorene (one or two layers). The scanning rate of AFM is slow compared to the fast degradation of very-few-layer phosphorene in ambient conditions and AFM can easily generate an error of one or even two layers, owing to the large surface roughness in very-few-layer phosphorene samples. AFM can also introduce potential contaminants that might affect further characterizations on the same sample. Unlike in TMD semiconductors, where Raman mode frequency has a monotonic dependence on the layer number, phosphorene has a non-monotonic dependence owing to the complicated Davydov-related effects[18]. Moreover, the relatively high-power laser used in Raman spectroscopy can significantly damage the phosphorene samples.

To overcome the aforementioned challenges, we propose and implement a rapid, noninvasive, and highly accurate approach to determine the layer number by using optical interferometry (Figure 1). Specifically, we measure the optical path length (OPL) of the light reflected from the phosphorene that was mechanically exfoliated onto a SiO_2/Si substrate (275 nm thermal oxide). The OPL is determined from the relation: $OPL_{BP} = -\frac{\lambda}{2\pi}(\phi_{BP} - \phi_{SiO_2})$, where λ is the wavelength of the light source and is equal to 535 nm, and ϕ_{BP} and

ϕ_{SiO_2} are the phase shifts of the light reflected from the phosphorene flake and the SiO_2/Si substrate (Figure 1c inset), respectively. The direct relationship between the OPL and the layer number is firmly established by a first-principle calculation and experimental calibration, as shown in Figure 1d. Even though the thickness of monolayer phosphorene is less than 1 nm, its OPL is larger than 20 nm owing to the multiple interfacial light reflections (Supplementary Information). That is, the virtual thickness of a phosphorene flake is amplified by more than 20 times in the optical interferometry, making the flakes easily identifiable. In the experiment, phase-shifting interferometry (PSI) is used to measure the OPL by analyzing the digitized interference pattern. In contrast to the highly focused and relatively high-power laser used in Raman system, PSI uses almost non-focused and very low-density light from a light-emitting diode (LED) source to achieve fast imaging (Supplementary Information), which inflicts no damage to the phosphorene samples. The step change of the OPL is ~20 nm for each additional phosphorene layer, as indicated by the red dots in Figure 1d. Considering that the accuracy of the instrument is ~0.1 nm, a step change of 20 nm yields extremely robust identification of the layer number. Statistical OPL values for phosphorene from mono- to six-layer (1L to 6L) were collected and at least five different samples were measured with the PSI system for each layer number. The measured OPL values agree very well with our theoretical calculations (Figure 1d). Recently, we also successfully used PSI to quickly and precisely identify the layer numbers of TMD atomically thin semiconductors[21].

Subsequent to PSI measurement, the sample was placed into a Linkam THMS 600 chamber, at a temperature of −10 ℃ with a slow flow of nitrogen gas to prevent degradation of the sample[8]. The low temperature (−10 ℃) is a very crucial factor because it can freeze the moisture in the chamber and significantly delay the sample degradation. Under −10 ℃ and nitrogen protection, monolayer phosphorene samples can survive for several hours in the chamber. However, even in a temperature of −10 ℃ with nitrogen gas protection, the monolayer phosphorene sample was found damaged when the power of the pulsed laser was higher than 1.15 μW (Supplementary Fig. S3). When the chamber temperature was raised from −10 ℃ to room temperature, the monolayer phosphorene was oxidized immediately and the PL signal disappeared. In contrast to monolayer phosphorene, 2L and 3L phosphorene samples can survive for more than 15 hours under −10 ℃ and for several hours when the chamber temperature was raised to room temperature.

Because of the strongly layer-dependent peak energies and the direct band gap nature of phosphorene, we are able to further confirm the layer number identification by measuring their corresponding peak energies of the PL emission (Figure 2). Figure 2a shows the normalized PL spectra of the mono- to five-layer phosphorene samples. The emission peak of the PL spectrum for monolayer phosphorene is at 711 nm, corresponding to a peak energy of 1.75 eV. This PL peak energy value was measured at −10 ℃ and it is expected not to vary too much at room temperature. Temperature-dependent PL measurements were conducted on 2L and 3L phosphorene samples from 20 ℃ down to −70 ℃; very minor shifts of –0.112 meV ℃$^{-1}$ and –0.032 meV ℃$^{-1}$ with temperature were observed for 2L and 3L phosphorene samples, respectively (Supplementary Fig. S4). Assuming a similar low temperature dependence for monolayer phosphorene, its PL peak energy at room temperature would be only ~1–4 meV lower than the measured value at −10 ℃. Combining the results of our previous work[8] on few-layer phosphorene (2L to 5L) with the results obtained from our recent samples (1L to 5L), it can be clearly observed that the peak energy of PL
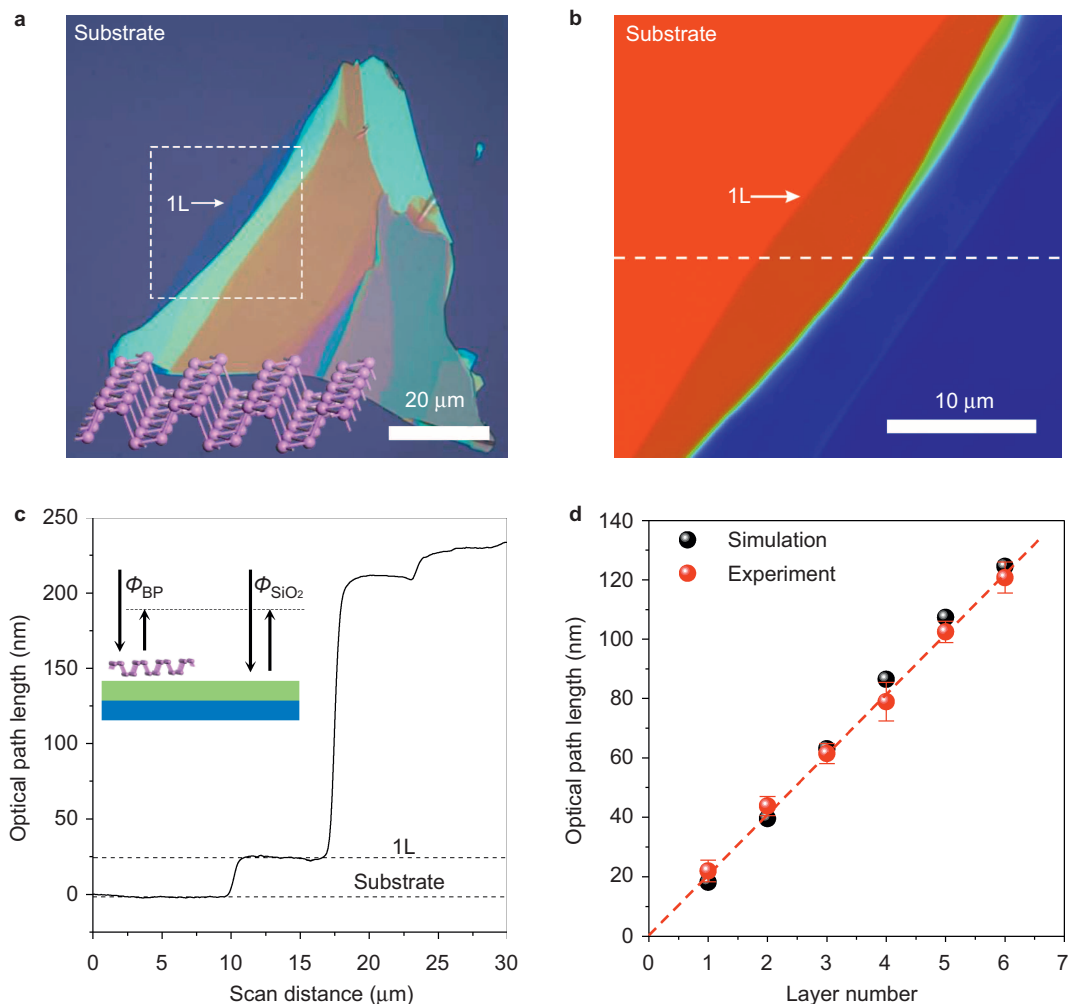
Figure 1 Robust identification of mono- and few-layer phosphorene by PSI. (**a**) Optical microscope image of a monolayer phosphorene (labeled as "1L"). Inset is the schematic of single-layer phosphorene molecular structure. (**b**) PSI image of the dash line box area indicated in **a**. (**c**) PSI measured OPL values along the dash line indicated in **b**. Inset is the schematic plot showing the PSI measured phase shifts of the reflected light from the phosphorene flake (ϕ_{BP}) and the SiO_2/Si substrate (ϕ_{SiO_2}). (**d**) OPL values from simulation and experiment PSI measurements for phosphorene samples from 1L to 6L. For each layer number of phosphorene, at least five different samples were characterized for the statistical measurements. The red dash line is the linear trend for statistical data measured with the PSI system.

emission shows unambiguous layer dependence (Figure 2b). For each layer number, at least three samples were characterized; the measured peak energies for 1L to 5L phosphorene are 1.75 ± 0.04, 1.29 ± 0.03, 0.97 ± 0.02, 0.84 ± 0.02, and 0.80 ± 0.02 eV, respectively. The PL emission energy of the phosphorene samples with higher layer number (>5) is beyond the measurement wavelength range (up to 1600 nm) of our system.

The peak energy of PL emission, also termed as optical gap (E_{opt}), is the difference between the electronic band gap (E_g) and the exciton binding energy (E_b) (Figure 2b inset). Owing to the strong quantum confinement effect, free-standing monolayer phosphorene is expected to have a large exciton binding energy of ~ 0.8 eV[9,15], whereas this value is expected to be only ~ 0.3 eV for monolayer phosphorene on a SiO_2/Si substrate because of the increased screening from the substrate[15]. If we use the measured electronic energy gap of ~ 2.05 eV by Pan *et al.*[22] using scanning tunneling spectroscopy and our measured optical gap of 1.75 eV in monolayer phosphorene, the exciton binding energy of monolayer phosphorene on SiO_2/Si substrate is determined to be ~ 0.3 eV, which agrees very well with the

prediction[15]. The optical gaps in phosphorene increase rapidly with decreasing layer number because of the strong quantum confinement effect and the van der Waals interactions between the neighboring sheets in few-layer phosphorene[9,23]. We used a power law form to fit the experimental data and obtained the fitting curve of $E_{opt} = \dfrac{1.486}{N^{0.686}} + 0.295$, where E_{opt} is the optical gap in unit of eV and N is the layer number (Figure 2b). The layer-dependent optical gaps, as indicated in Figure 2b, agree very well with the theoretical predictions[7,9]. For bulk phosphorene sample with large N value, its optical gap approaches the limit value of ~ 0.295 eV, which matches very well with the measured energy gap (~ 0.3 eV) of bulk phosphorene[5,24]. Previously, Ye *et al.*[1] observed bright exciton PL emission at ~ 1.45 eV from a monolayer phosphorene that is coated with a protection layer of PMMA. This protection layer might introduce some defect states to the sample, which could change the PL emission energy. Our samples have no any protection layers and we did not use any chemical treatment processes, which provide very clean surfaces in our samples for exciton nature investigations.
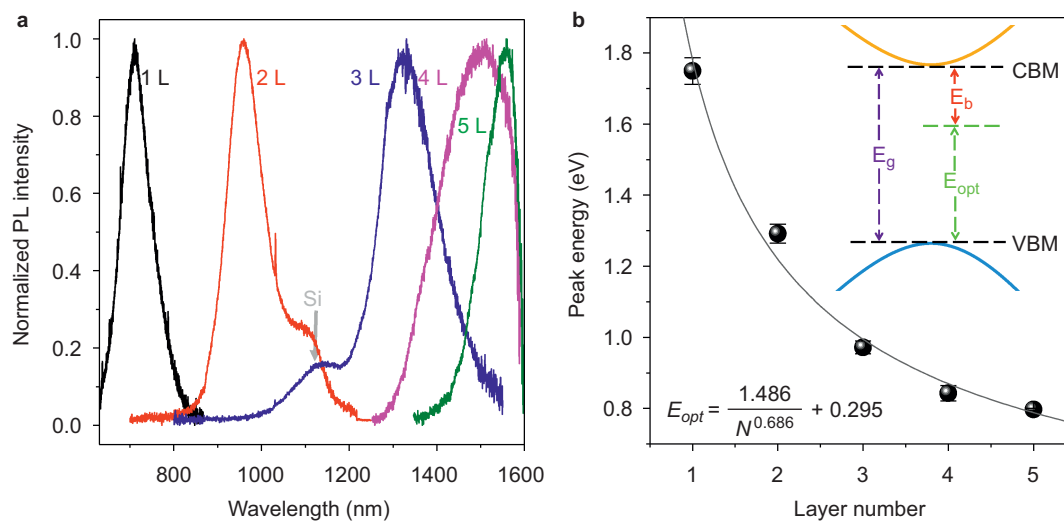
Figure 2 PL characteristics of mono- and few-layer phosphorene. (**a**) PL spectra of the mono- to five-layer phosphorene samples. Each PL spectra is normalized to its peak intensity and system background. (**b**) Evolution of PL peak energy with layer number of phosphorene from experimental PL spectra, showing a rapid increase in peak energy as the layer number decreases. The solid gray line is the fitting curve $E_{opt} = \frac{1.486}{N^{0.686}} + 0.295$, where E_{opt} is the optical gap in unit of eV and N is the layer number. Note: the PL for the monolayer phosphorene was measured at $-10\,°C$, while others were measured at room temperature. For monolayer phosphorene, the difference between PL peak energies at $-10\,°C$ and at room temperature is estimated to be less than 5 meV. Inset: schematic energy diagram showing the electronic band gap (E_g), and the exciton binding energy (E_b).

The dynamics of excitons and trions have been of considerable interest for fundamental studies of many-body interactions[13,14], such as carrier multiplication and Wigner crystallization[25]. Monolayer phosphorene, whose excitons are predicted to be confined in a quasi-one-dimensional (1D) space[7,9], provides an ideal platform for investigating remarkable exciton and trion dynamics in a reduced dimension. Here, we successfully probed the exciton and trion dynamics in monolayer phosphorene by controlling the photo-carrier injection in power-dependent PL measurements (Figure 3). The measured PL spectra exhibit two clear peaks with central wavelengths at ~705 nm (labeled as "A") and ~760 nm (labeled as "X"), whose intensities and peak positions are highly dependent on the excitation power (Figure 3a). We used Lorentzian curves to fit the measured PL spectra and extracted the spectral components of these two peaks, indicated by red and blue curves in Figure 3a. The intensity of higher energy peak A increases almost linearly with laser power (Figure 3b), while that of lower energy peak X gradually saturates at a relatively high photo-carrier injection. When the excitation power changed from 0.19 to 1.15 μW (Figure 3c), the optical gap of A emission (E_A) monotonically decreased by ~15 meV, while that of X emission (E_X) increased by ~35 meV. The higher energy peak A is attributed to exciton emission. The measured full width at half maximum (FWHM) of peak A decreases with increase in excitation power (Supplementary Fig. S5a), which suggests an increase in the exciton binding energy, and thus, a reduction in E_A with the increase in power within the range of our experiments[26,27]. Owing to the appropriate protection for the phosphorene, we obtained very stable PL spectra data and the measurement errors of the exciton and trion energies are minimized to be ~5 meV (Supplementary Table S1).

The origin of peak X is particularly interesting. We believe the experimental observations do not support that peak X comes from the emission of localized excitons[28,29]. First, the energy difference between the PL emissions from the localized and free excitons is not sensitive to the relatively low density of photo-carrier injection[28,29]. But in our experiment, this energy difference decreases significantly from ~150 meV to ~100 meV when the power of excitation laser increases from 0.19 to 1.15 μW. Furthermore, localized excitons are expected to have a longer lifetime than free excitons because of the localization effect of squeezing an exciton in the zero-dimension-like state[28,30]. However, our TRPL measurements revealed that the carrier lifetime from X state is less than that from A state (discussed later). On the other hand, the origin of X state can be attributed to trions[13,14]. The trion peak intensity saturates at high photo-carrier injection (Figure 3b) because the free carriers coming from initial doping are almost depleted during the formation of trions. The trion density estimated from our optical injection is comparable to the estimated initial doping level of our monolayer phosphorene sample (Supplementary Information).

The difference between the peak energies of exciton and trion PL emission is predicted to be[13,31]:

$$E_A - E_X = E_{Tb} + \varDelta E \qquad (1)$$

where E_{Tb} is the binding energy of trions and $\varDelta E$ is the average energy needed to add one carrier into the free-carrier system. The energy difference $E_A - E_X$ represents the minimum energy for the removal of one electron (hole) from a negative (positive) trion. To convert a trion to an exciton, one of the two electrons (holes) in the negative (positive) trion will be unbound first ($+E_{Tb}$) and then added into the system ($+\varDelta E$)[13,31]. During PL excitation, the same amount of electrons and holes will be injected into the conduction band and valence band, respectively. At low excitation power (power close to zero), the system is in an equilibrium state and $\varDelta E$ is approximately equal to the Fermi energy E_F that is determined at the initial doping level[13,31]. At higher PL excitation power with more carrier injection, the initial doping becomes less important because of the enhanced screening effect from the injected photo-carriers. In most conventional PL measurements with very high excitation power[10,14,32], $\varDelta E$ can be neglected and the trion binding energy can be approximately taken as the energy difference $E_A - E_X$. Here, we used a very low power range as the PL
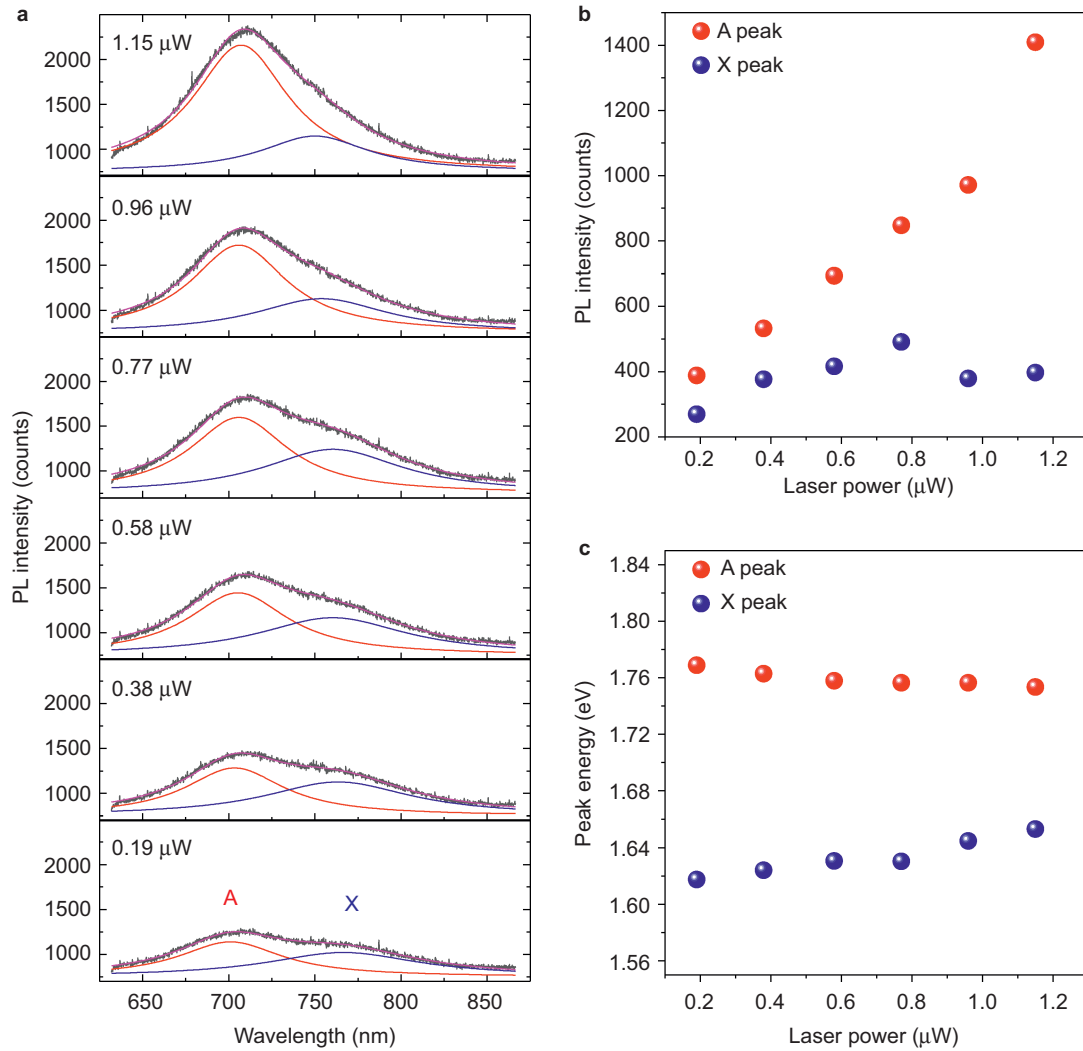
Figure 3 Exciton and trion dynamics in monolayer phosphorene. (**a**) Measured PL spectra (solid gray lines) under various excitation laser power. PL spectra are fit to Lorentzians (solid red lines are the exciton components, solid blue lines are the trion components, and solid pink lines are the cumulative fitting results). (**b**) PL intensity of exciton (A) and trion (X) as a function of laser power. (**c**) PL peak energy of exciton (A) and trion (X) as a function of laser power.

excitation and were able to observe the unique effect of ΔE. We started with a low power excitation at 0.19 μW, which has an injected photocarrier concentration comparable to the initial doping level. As we increased the excitation power, the energy difference $E_A - E_X$ decreased, indicating a reduction of ΔE. At high excitation power (1.15 μW), the initial doping becomes less important and ΔE can be approximately neglected; the energy difference $E_A - E_X$ of ∼100 meV at high excitation power (1.15 μW) can be taken to be the upper limit of the trion binding energy in monolayer phosphorene. This value agrees well with the estimated trion binding energy in monolayer phosphorene of $E_{\mathrm{Tb}} \sim 0.3 E_b$[10,23] and the calculated exciton binding energy in monolayer phosphorene on SiO$_2$/Si substrate is $E_b \sim 0.3$ eV[9]. In monolayer phosphorene, both positive and negative trions are expected to have similar binding energies, since the effective masses of electrons and holes are almost equal[7,9].

Carrier lifetime has been considered to be a very critical parameter in semiconducting materials[33–35]. The accurate probing of the carrier lifetime in monolayer phosphorene can greatly help us in understanding its highly excitonic nature and to better explore its optoelectronic

applications. In order to understand the origin of X emission peak, we used TRPL to characterize the carrier lifetimes of these two different states, A and X. For the first time, we successfully measured the carrier lifetime of the A peak emission in monolayer phosphorene at 220 ± 8 ps. The carrier lifetime of the X peak emission was found to be lower than the resolution of our system (∼40 ps), which confirms the aforementioned reasoning that X peak should not be from the emission of localized excitons. In our experiments, a linearly polarized pulse laser (frequency doubled to 522 nm, with 300 fs pulse width and 20.8 MHz repetition rate) was used to excite the monolayer phosphorene samples. PL signal was collected by a grating spectrometer and the PL intensity decay was detected using a Si SPAD and the TCSPC (PicoHarp 300) system. The measured PL decay of the exciton peak of our monolayer phosphorene sample with a laser power of 1.15 μW is presented in Figure 4a with the system response to the excitation laser as reference. We fitted the measured decay curve with equation $I_{BP} = A\exp\left(-\dfrac{t}{\tau}\right) + B$, where I_{BP} is the PL intensity, A and B are two constants, t is time, and τ is carrier lifetime. Through fitting, the carrier
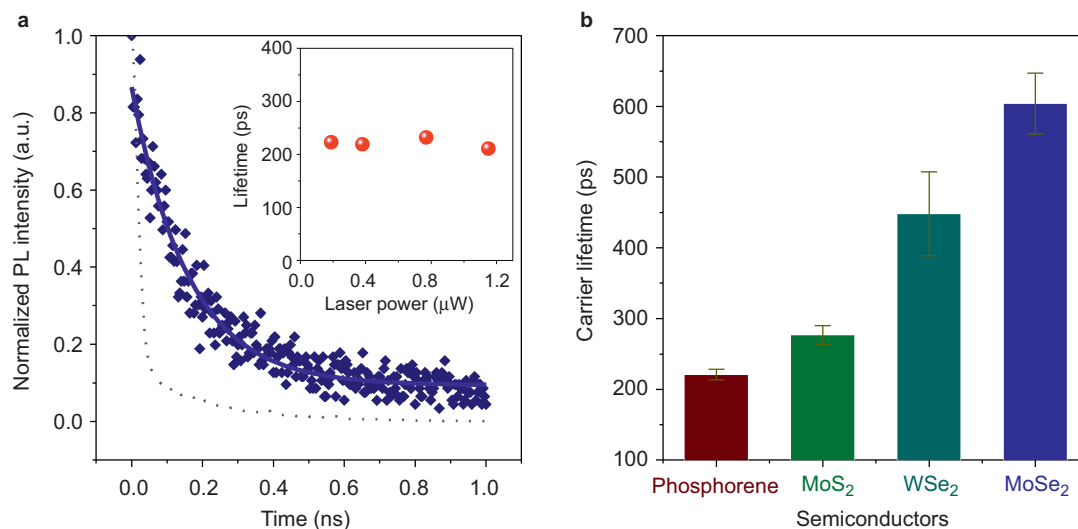
Figure 4 TRPL characteristics of monolayer phosphorene. (**a**) PL decay profile of the exciton peak in monolayer phosphorene, by using a pulse 522 nm (frequency doubled) excitation laser at a laser power of 1.15 μW and a TCSPC. A lifetime of 211 ps can be extracted from the PL decay curve by exponential fitting. The blue solid line curve is the exponential fitting of the experimental data and the gray dash line curve is the instrument response to the excitation laser pulse. Inset shows the power-dependent carrier lifetime of monolayer phosphorene at pump laser power of 0.19, 0.38, 0.77, and 1.15 μW. For different excitation laser power, the carrier lifetime of monolayer phosphorene stays ~ 220 ps and shows no significant power dependence. (**b**) Carrier lifetime for excitons of monolayer phosphorene, MoS_2, WSe_2, and $MoSe_2$ semiconductors. All data were measured with a pulse 522 nm excitation laser and with a laser power of 1.15 μW.

lifetime τ was determined to be 211 ps. Power-dependent PL decay was conducted with pulse laser powers 0.19, 0.38, 0.77, and 1.15 μW, and the same fitting process was performed to obtain the carrier lifetimes to be 222, 219, 232, and 211 ps, respectively, showing no significant power dependence. The power-dependent carrier lifetime measurement results of the monolayer phosphorene sample differ from the results of other TMD semiconductors, which show a decreasing carrier lifetime with increase in excitation laser power[35]. This independence of carrier lifetime of our monolayer phosphorene samples suggests that higher order processes such as exciton–exciton annihilation were negligible for the excitation power employed in our experiments[34]. We also compared the carrier lifetime data from monolayer phosphorene samples with those from other monolayer TMD semiconductors measured with the same system, as indicated in Figure 4b. The carrier lifetime values for monolayer phosphorene, MoS_2, WSe_2, and $MoSe_2$ were measured to be 221 ± 8, 277 ± 13, 448 ± 60, and 604 ± 43 ps, respectively.

CONCLUSIONS

In conclusion, we report a rapid, noninvasive, and highly accurate approach to determine the layer number of mono- and few-layer phosphorene using PSI. The identification is further confirmed by reliable, highly layer-dependent PL peak energies. These two methods provide definite references for future mono- and few-layer phosphorene layer number identification. The dynamics of excitons and trions in monolayer phosphorene was successfully characterized by controlling the photo-carrier injection in a relatively low excitation power range. Based on the measured optical gap and previously measured electronic energy gap, we determined the exciton binding energy to be ~0.3 eV for the monolayer phosphorene on SiO_2/Si substrate, which agrees well with theoretical predictions. A huge trion binding energy of ~100 meV (upper limit) was first observed in monolayer phosphorene on SiO_2/Si substrate. In addition, a carrier lifetime of 220 ps for the monolayer phosphorene was first measured, which is comparable to

other 2D TMD semiconductors. Our results open new routes for both the investigation of 2D quantum limit in reduced dimensions and development of novel optoelectronic devices.

AUTHORS' CONTRIBUTIONS

Yuerui Lu designed the project; Jiong Yang did the PL measurements, data analysis and TMD semiconductor sample preparation; Renjing Xu conducted PL data fitting analysis, few-layer phosphorene sample preparation and part of the theoretical calculations; Jiajie Pei conducted the preparation of monolayer phosphorene and PSI measurements; Ye Win Myint contributed to sample preparation; Fan Wang built the optical characterization setup; Zhu Wang and Zongfu Yu performed the theoretical simulations for the OPL of phosphorene. All authors contributed to the manuscript.

1 Liu H, Neal AT, Zhu Z, Luo Z, Xu X *et al*. Phosphorene: an unexplored 2D semiconductor with a high hole mobility. *ACS Nano* 2014; **8**: 4033–4041.
2 Buscema M, Groenendijk DJ, Blanter SI, Steele GA, van der Zant HS *et al*. Fast and broadband photoresponse of few-layer black phosphorus field-effect transistors. *Nano Lett* 2014; **14**: 3347–3352.
3 Fei R, Yang L. Strain-engineering the anisotropic electrical conductance of few-layer black phosphorus. *Nano Lett* 2014; **14**: 2884–2889.
4 Xia F, Wang H, Jia Y. Rediscovering black phosphorus as an anisotropic layered material for optoelectronics and electronics. *Nat Commun* 2014; **5**: 4458.
5 Li L, Yu Y, Ye GJ, Ge Q, Ou X *et al*. Black phosphorus field-effect transistors. *Nat Nanotechnol* 2014; **9**: 372–377.

doi:10.1038/lsa.2015.85

6   Hong T, Chamlagain B, Lin W, Chuang HJ, Pan M *et al*. Polarized photocurrent response in black phosphorus field-effect transistors. *Nanoscale* 2014; **6**: 8978–8983.

7   Qiao J, Kong X, Hu ZX, Yang F, Ji W. High-mobility transport anisotropy and linear dichroism in few-layer black phosphorus. *Nat Commun* 2014; **5**: 4475.

8   Zhang S, Yang J, Xu R, Wang F, Li W *et al*. Extraordinary photoluminescence and strong temperature/angle-dependent Raman responses in few-layer phosphorene. *ACS Nano* 2014; **8**: 9590–9596.

9   Tran V, Soklaski R, Liang Y, Yang L. Layer-controlled band gap and anisotropic excitons in few-layer black phosphorus. *Phys Rev B* 2014; **89**: 235319.

10 Zhang S, Xu R, Wang F, Yang J, Wang Z *et al*. Extraordinarily bound quasi-one-dimensional trions in two-dimensional phosphorene atomic semiconductors. arXiv:1411.6124.

11 Geim AK, Novoselov KS. The rise of graphene. *Nat Mater* 2007; **6**: 183–191.

12 Radisavljevic B, Radenovic A, Brivio J, Giacometti V, Kis A. Single-layer MoS_2 transistors. *Nat Nanotechnol* 2011; **6**: 147–150.

13 Mak KF, He K, Lee C, Lee GH, Hone J *et al*. Tightly bound trions in monolayer MoS_2. *Nat Mater* 2013; **12**: 207–211.

14 Ross JS, Wu S, Yu H, Ghimire NJ, Jones AM *et al*. Electrical control of neutral and charged excitons in a monolayer semiconductor. *Nat Commun* 2013; **4**: 1474.

15 Rodin AS, Carvalho A, Neto AH. Excitons in anisotropic two-dimensional semiconducting crystals. *Phys Rev B* 2014; **90**: 075429.

16 Castellanos-Gomez A, Vicarelli L, Prada E, Island JO, Narasimha-Acharya KL *et al*. Isolation and characterization of few-layer black phosphorus. *2D Materials* 2014; **1**: 025001.

17 Wang X, Jones AM, Seyler KL, Tran V, Jia Y *et al*. Highly anisotropic and robust excitons in monolayer black phosphorus. *Nature Nanotechnol* 2015; **10**: 517–521.

18 Favron A, Gaufrès E, Fossard F, Lévesque PL, Phaneuf-L'Heureux AL *et al*. Exfoliating pristine black phosphorus down to the monolayer: photo-oxidation and electronic confinement effects. arXiv:1408.0345.

19 Liu V, Fan S. S^4: a free electromagnetic solver for layered periodic structures. *Comput Phys Commun* 2012; **183**: 2233–2244.

20 Li H, Zhang Q, Yap CC, Tay BK, Edwin TH *et al*. From bulk to monolayer MoS_2: evolution of Raman scattering. *Adv Funct Mater* 2012; **22**: 1385–1390.

21 Yang J, Wang Z, Wang F, Xu R, Tao J *et al*. Atomically thin optical lenses and gratings. arXiv:1411.6200.

22 Liang L, Wang J, Lin W, Sumpter BG, Meunier V *et al*. Electronic bandgap and edge reconstruction in phosphorene materials. *Nano Lett* 2014; **14**: 6400–6406.

23 Thilagam A. Two-dimensional charged-exciton complexes. *Phys Rev B* 1997; **55**: 7804–7808.

24 Keyes RW. The electrical properties of black phosphorus. *Phys Rev* 1953; **92**: 580–584.

25 Wigner E. On the interaction of electrons in metals. *Phys Rev* 1934; **46**: 1002–1011.

26 Yoshikawa M, Kunzer M, Wagner J, Obloh H, Schlotter P *et al*. Band-gap renormalization and band filling in Si-doped GaN films studied by photoluminescence spectroscopy. *J Appl Phys* 1999; **86**: 4400–4402.

27 Mu X, Zotova IB, Ding YJ, Yang H, Salamo GJ. Observation of an anomalously large blueshift of the photoluminescence peak and evidence of band-gap renormalization in InP/InAs/InP quantum wires. *Appl Phys Lett* 2001; **79**: 1091–1093.

28 Miyauchi Y, Iwamura M, Mouri S, Kawazoe T, Ohtsu M *et al*. Brightening of excitons in carbon nanotubes on dimensionality modification. *Nat Photonics* 2013; **7**: 715–719.

29 Iwamura M, Akizuki N, Miyauchi Y, Mouri S, Shaver J *et al*. Nonlinear photoluminescence spectroscopy of carbon nanotubes with localized exciton states. *ACS Nano* 2014; **8**: 11254–11260.

30 Wang H, Zhang C, Chan W, Manolatou C, Tiwari S *et al*. Radiative lifetimes of excitons and trions in monolayers of metal dichalcogenide MoS_2. arXiv:1409.3996.

31 Huard V, Cox RT, Saminadayar K, Arnoult A, Tatarenko S. Bound states in optical absorption of semiconductor quantum wells containing a two-dimensional electron gas. *Phys Rev Lett* 2000; **84**: 187–190.

32 Kheng K, Cox RT, d' Aubigné MY, Bassani F, Saminadayar K *et al*. Observation of negatively charged excitons X. in semiconductor quantum wells. *Phys Rev Lett* 1993; **71**: 1752–1755.

33 Mai C, Barrette A, Yu Y, Semenov YG, Kim KW *et al*. Many-body effects in valleytronics: direct measurement of valley lifetimes in single-layer MoS_2. *Nano Lett* 2013; **14**: 202–206.

34 Shi H, Yan R, Bertolazzi S, Brivio J, Gao B *et al*. Exciton dynamics in suspended monolayer and few-layer MoS_2 2D crystals. *ACS Nano* 2012; **7**: 1072–1080.

35 Salehzadeh O, Tran NH, Liu X, Shih I, Mi Z. Exciton kinetics, quantum efficiency, and efficiency droop of monolayer MoS_2 light-emitting devices. *Nano Lett* 2014; **14**: 4125–4130.